Scintillation Measurements of Broadband 980nm Laser Light in Clear Air Turbulence

F.M. Davidson[a], S. Bucaille[a], C. Gilbreath[b], E. Oh[b]

[a]Johns Hopkins University, Department of Electrical and Computer Engineering, 3400 N. Charles Street, Baltimore, MD 21218
[b]Naval Research Laboratory, 4555 Overlook Ave., SW, Remote Sensing Division, Code 7215, Washington, DC 20375

Abstract

Intensity scintillation variances and intensity probability density functions (PDF) were experimentally measured for broad-band (2nm), 980 nm laser light reflected by two corner-cube retro-reflectors as a function of retro-reflector lateral spacing over a short (75 m) atmospheric optical path. The PDFs transitioned from broad double peaked "beta –shaped" densities to log-normal ones as the retro-reflector spacing was increased to exceed the optical field lateral coherence length. Specific spacing for a given average atmospheric refractive index structure constant C_n^2 eliminated coherent interference between light beams returned by each retro-reflector.

Keywords: Optical communications, coherence, atmospheric optics, turbulence

I. Introduction

High power, low coherence volume lasers are useful in free-space atmospheric optical communication links. For some applications, retro-modulators can be useful for optical terminals in asymmetric links [1, 2]. In applications typically requiring transmission over longer ranges, an array of devices is sometimes necessary for a wider field-of-regard to close a given link. However, in applications where compact arrays are required, partial coherence can cause performance losses due to interference effects between co-located retro-reflectors.

For such a link propagating in the atmosphere, two effects can contribute to channel degradation. The first is scintillation and turbulence and the second is the effects of partial coherence. The latter manifests as constructive or destructive interference of the intensity-modulated light reflected from each element in the retro-reflector array. In order to mitigate this effect, each retro-reflector should be located in a different coherence volume of the transmitted light beam. Otherwise, additional intensity fluctuations due to the coherent interference between the retro-reflected light beams will be present in the returned beam. This effect will combine with scintillations induced by atmospheric turbulence and further degrade performance beyond the level caused by the turbulence alone. This problem sets the stage for our initial investigation in how to characterize and separate out these fects through such a channel. The use of high power, broad line-width (~ 2 nm) 980 nm laser diodes is particularly attractive for this application. The very small coherence volume associated with such

Free-Space Laser Communication and Active Laser Illumination III,
edited by David G. Voelz, Jennifer C. Ricklin, Proc. of SPIE Vol. 5160
(SPIE, Bellingham, WA, 2004) · 0277-786X/04/$15 · doi: 10.1117/12.504863

Report Documentation Page

Form Approved
OMB No. 0704-0188

1. REPORT DATE	2. REPORT TYPE	3. DATES COVERED
2004		**00-00-2004 to 00-00-2004**

4. TITLE AND SUBTITLE	5a. CONTRACT NUMBER
Scintillation Measurements of Broadband 980nm Laser Light in Clear Air Turbulence	5b. GRANT NUMBER
	5c. PROGRAM ELEMENT NUMBER
6. AUTHOR(S)	5d. PROJECT NUMBER
	5e. TASK NUMBER
	5f. WORK UNIT NUMBER
7. PERFORMING ORGANIZATION NAME(S) AND ADDRESS(ES) **Naval Research Laboratory,Code 7215,4555 Overlook Avenue, SW,Washington,DC,20375**	8. PERFORMING ORGANIZATION REPORT NUMBER
9. SPONSORING/MONITORING AGENCY NAME(S) AND ADDRESS(ES)	10. SPONSOR/MONITOR'S ACRONYM(S)
	11. SPONSOR/MONITOR'S REPORT NUMBER(S)

12. DISTRIBUTION/AVAILABILITY STATEMENT
Approved for public release; distribution unlimited

13. SUPPLEMENTARY NOTES

14. ABSTRACT

15. SUBJECT TERMS

16. SECURITY CLASSIFICATION OF:			17. LIMITATION OF ABSTRACT	18. NUMBER OF PAGES	19a. NAME OF RESPONSIBLE PERSON
a. REPORT **unclassified**	b. ABSTRACT **unclassified**	c. THIS PAGE **unclassified**		**12**	

lasers makes it possible to closely space the individual retro-reflectors while still locating them in separate coherence cells.

This paper reports the results of experimental measurements of intensity scintillation levels of 980 nm, 2nm band-width laser light propagated through the turbulent atmosphere as a function of retro-reflector spacing in a plane normal to the direction of laser beam propagation over a horizontal optical path up to 100 m in length. Intensity probability density functions (PDF) were measured for the returned light reflected by a single retro-reflector and by a pair of retro-reflectors equally spaced from the laser beam center. The results indicted that for a sufficiently large spacing between two or retro-reflectors, the intensity PDFs were always log-normal. In the case of two closely spaced retro-reflectors, the intensity PDFs were "U" shaped (or beta-shaped) densities [3] that eventually became log-normal as the retro spacing increased to the point where the optical fields reflected from each became statistically independent of each other.

II. Experimental Measurements

Figure 1 shows a picture of the laser transmitter and collimator, beam splitter, turning mirror, focusing lens and aperture stop, and photodiode/transimpedance current amplifier combination (Thor Labs PDA 400). Light from the 980 nm laser diode source was single mode fiber coupled to the collimator lens and directed to the target array of retro-reflectors by passing through a 50/50 beam splitter. The beam splitter redirected light reflected by the retro-reflectors to a 2 in diameter, 10 cm focal length lens via the turning mirror. The focusing lens effective aperture was controlled with the use of an iris diaphragm of 2.5mm to 45mm adjustable opening. The PDA 400 was operated at its maximum gain setting of 750 Kv/amp and background light was eliminated with the use of a 10 nm bandpass interference filter. The electrical bandwidth was 50 Khz and the responsivity, *R*, of the photodiode was 0.65 amps/watt at 980 nm. The output voltage was sampled by a National Instruments data acquisition board at the rate of 10^4 10-bit samples per second for up to ten seconds and the digitized values stored in data files on a portable computer.

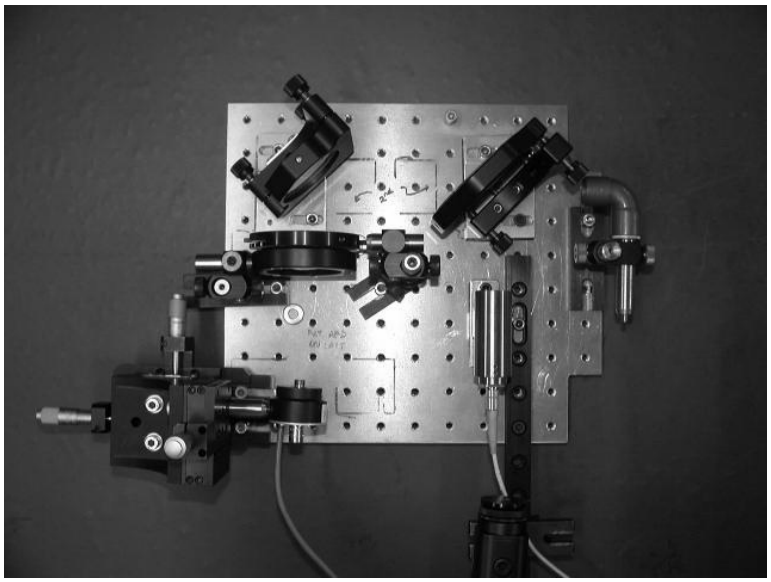

Figure 1. Photograph of the measurement apparatus

The 2 nm bandwidth of the 980 nm laser gives a laser temporal coherence time of $\tau = (\lambda^2/c\Delta\lambda) =$ 1.6 x10^{-12} sec or a coherence length of $l_{coh} = c\tau = 0.5$ mm. Measurements of the angular divergence of the collimated laser beam yielded a value of about 1 mrad. The diameter of the individual retro-reflectors was 6 mm. At one-way path lengths of 50 -100 m, the beam diameter was on the order of 10 to 20 cm.

In order to obtain interference between the light reflected from two retro-reflectors, the optical path length difference must be kept less than 0.5 mm, the longitudinal coherence length of the laser. This required mounting the retro-reflectors on a flat target board and aligning the plane of the target board to within less than one degree of the normal to the incident beam propagation direction. A large flat mirror was mounted flat on the target board immediately adjacent to the center retro-reflector. The board itself could be rotated about two axes normal to the direction of beam propagation. A CCD camera mounted on the transmitter board was used to detect both the reflections from the corner cube retro-reflectors and the flat mirror. The reflection from the retro-reflectors was used to center the transmitted laser beam on the array of retro-reflectors. The target board was aligned so that the flat mirror reflected the incident laser beam back onto the beam splitter on the transmitter board thereby assuring the plane of the target board was normal to the beam propagation direction to high accuracy (less than one degree of misalignment). Once the target board was aligned, the flat mirror was covered so that only the retro-reflectors were illuminated.

The atmospheric path lengths used had to be kept relatively short because of the limited power output of the 980 nm diode lasers used (100mW or 300mW), small areas of the retro-reflectors, and 6dB power loss due to the beam splitter. The latter could in principle be eliminated through the use of a polarization state sensitive beam splitter and quarter wave plate. The corner cube retro-reflectors however alter the polarization state of the reflected beam so this was not feasible. Another alternative was to replace the beam splitter with a hole coupled mirror that would transmit all the laser light but would not reflect the exact center of the return beam. In order to keep the interpretation of the results of the measurements as unambiguous as possible, neither of these alternatives was used. The atmospheric turbulence induced intensity scintillation levels, which increase as $C_n^2 k^{7/6} L^{11/6}$,[4] were therefore quite small and values of $\sigma_I^2/\langle I\rangle^2$ were typically in the range 10^{-3}. The ten bit quantization of the photo-detector output signals gave digital "quantization noise" variance values on the order of 10^{-5} . The lateral spatial coherence length, on the other hand, decreases with path length as $(C_n^2 k^2 L)^{-3/5}$ [4] and was typically a few centimeters. A scintillometer was used to measure values of the refractive index constant, C_n^2. The atmospheric path traversed a grassy area in full sun light. This typically gave measured values of C_n^2 in the range 10^{-13} to 10^{-14} $m^{-2/3}$. At a wavelength of 980 nm path lengths between 50 and 100 m resulted in easily measured values of normalized intensity scintillation and spatial coherence length.

The measurements consisted of the following. The PDA-400 output voltage waveform was digitized and recorded for ten second intervals (100,000 points) under the following conditions: for a fixed lens aperture size, data was recorded from a single retro-reflector located in the center of the beam, from two retro-reflectors symmetrically displaced from the beam center line by distance d (retro reflectors separated from each other by 2d. This procedure was repeated for receiver lens aperture diameters of 3 mm up to 30 mm. The normalized intensity variance and probability density function

(PDF) for normalized intensity values were computed for each data file. Spatial coherence lengths of the optical field at the target board could be found by observing the decrease in the normalized variance of the light returned by two retro reflectors as the separation between them increased. Measurements of the normalized intensity variance for light reflected by two or more retro reflectors can be used to infer bit error rate performance of an actual communication system. No measurements of bit error rates were made however, as the objective of this work was simply to determine the retro reflector spacing required for this type of laser and typical atmospheric turbulence conditions.

It was of course, not possible to control values of C_n^2 for these measurements. This required taking many data files and discarding those for which it was apparent that this parameter had changed substantially over the course of the ten seconds of data acquisition. This manifested itself in the form of PDFs that had many anomalous points and/or values of normalized intensity variances that changed substantially over one second long subsections within each data file. Nevertheless, there were frequent occasions when C_n^2 varied by less than a factor of two over tens of minutes.

III. Results

The voltage output by the PDA-400 is related to the photocurrent produced by the GaAs p-i-n photodiode as $v_0(t) = G_V i(t)$ where G_V is the trans-impedance gain, 750 Kv/amp. The photocurrent is related to the total optical power incident of the photodiode by $i(t) = RI(t) = (e\eta / hf)I(t)$ where R is the photodiode responsivity, e is the charge of one electron, η is the dimensionless quantum efficiency of the photodiode, and hf is the photon energy. The mean and variance of the output voltage are given by [5]

$$\langle v_0(t) \rangle = G_V R \int < I(t') > h(t - t')dt' \qquad (1)$$

$$\sigma_v^2 = G_V^2 eR \int < I(t') > h^2(t - t')dt' + G_V^2 R^2 \iint K(r,s)h(t - r)h(t - s)drds \qquad (2)$$

where all integrals extend from $-\infty, \infty$, $K(r,s) = < I(r)I(s) > - < I(r) >< I(s) >$ is the optical intensity covariance, and $h(t - t')$ is the impulse response function of the photo-diode trans-impedance amplifier combination which is causal and of sufficiently large bandwidth (50 Khz) that *K(r,s)* remains constant over the time scale over which $h(t - r)h(t - s) \neq 0$. Under these conditions, the normalized voltage variance becomes

$$\frac{\sigma_V^2}{< v >^2} = \frac{2Be}{R < I >} + \frac{\sigma_I^2}{< I >^2} \qquad (3)$$

where *2B* represents an effective bandwidth given by $\int h^2(t)dt / (\int h(t)dt)^2$. The first term on the right hand side of eqn. (3) represents the shot noise associated with the photodetection process and the second is the normalized variance of the light intensity fluctuations caused by the atmospheric turbulence. Measurements were made only under conditions when the average output voltage levels exceeded 0.1 V which corresponds to a value of $R < I >= 0.13\mu A$. An effective bandwidth of *2B* = 50 Khz gives a value of 6×10^{-8} for the shot noise contribution which is four or more orders of magnitude smaller than the turbulence induced expected values of normalized optical intensity variance. In the absence of optical intensity fluctuations, eqn. (3) reduces to just the variance due to

shot noise, i.e. the fluctuations in photocurrent due to the Poisson distributed number of photons in a constant intensity optical field.

In order to determine the PDF of the return light intensity, each recorded data file was processed as follows. First, the mean value of the ten bit digitized samples of PDA-400 output voltage was computed. A new data file was then created that consisted of "normalized data", that is, the original data points each divided by the mean, hereafter denoted as z_i. Next a histogram of the normalized data was computed with bin size $\Delta z = (5V/1024)/<v>$. The experimentally measured PDF for z was found by dividing the total number of occurrences of values of z_i in the range z_i, $z_i + \Delta z$ by the total number of data points in the file. The experimentally measured PDF was then plotted as a function of z with each data point located at $z_i + (\Delta z/2)$.

In order to compare the experimentally measured PDF with a log-normal PDF, a third data file consisting of the values $\ln(z_i)$ was created. The mean and variance of these data points were computed and then used in the theoretical expression for the log-normal PDF

$$p(z_i) = \frac{1}{\sqrt{2\pi\sigma^2_{\ln z}}} \frac{1}{z_i} \exp\left(- \frac{(\ln z_i - <\ln z>)^2}{2\sigma^2_{\ln z}} \right) \qquad (4)$$

A typical result for light reflected by a single retro-reflector located at the center of the beam is shown in Figure 2 where the experimentally determined points of the PDF lie very close to the curve predicted by eqn. (4). Points at the wings of the PDF that lie off the curve represent very few occurrences of those particular values of z_i. The actual number of events can be computed by multiplying the ordinate value by $(\Delta z)N$ where N is the total number of data points in the file, typically 10^5. For this figure these points represent 1 event at a PDF value of 10^{-3}. The measured variance $\sigma^2_{\ln z} = 2.58\text{x}10^{-3}$ for this beam divergence, beam waist and distance gives an inferred value of $C_n^2 = 2\text{x}10^{-14}$ m$^{-2/3}$ found by using the formulas in Table 2 of [6], a value well within the range of values registered by the scintillometer.

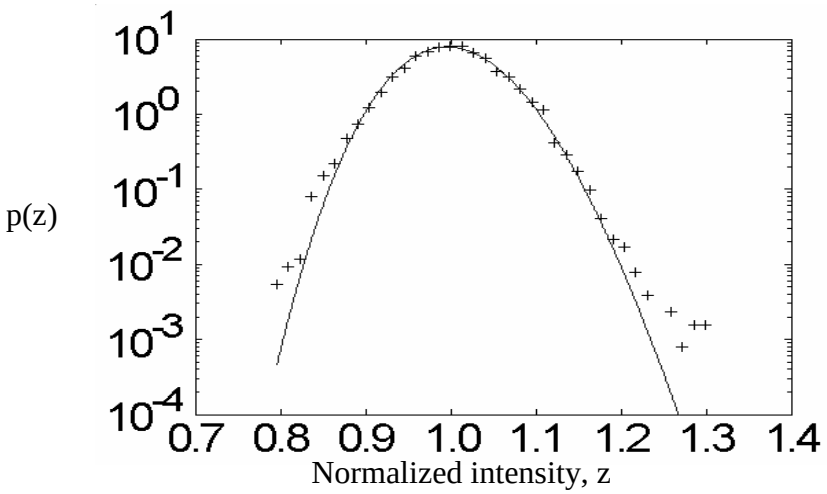

Figure 2. PDF(z) for light returned by a single retro-reflector; $\sigma^2_{\ln z} = 2.58\text{x}10^{-3}$, $\Delta z = 1.3x10^{-2}$

The PDF for light reflected by two closely spaced retro-reflectors is clearly not lognormal as shown by the data of Figures 3(a)-(d) which are plots of experimentally measured PDFs with receiver aperture diameter, D_R, as a parameter for a fixed retro-reflector spacing of 10 mm.

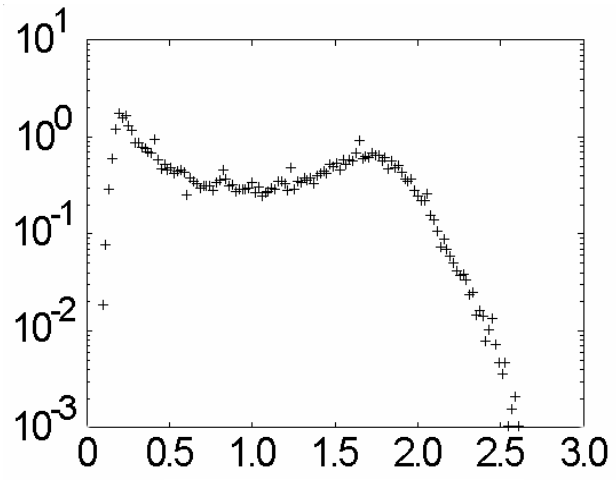

Fig. 3(a)

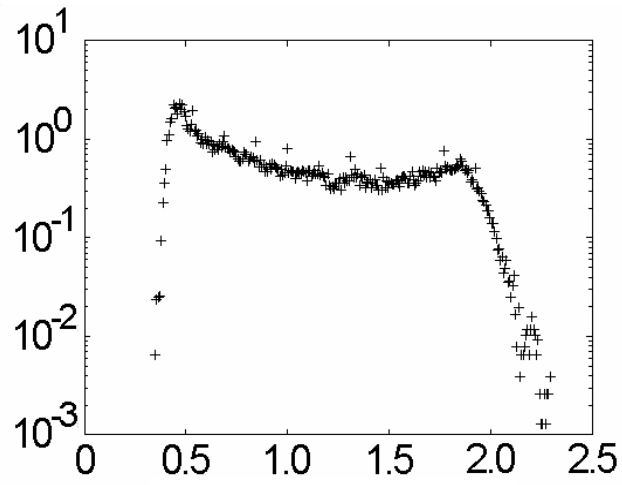

Fig. 3(b)

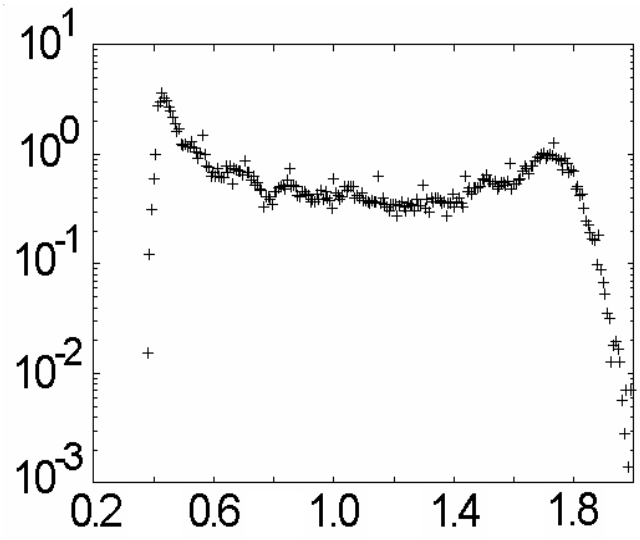

Fig. 3 (c)

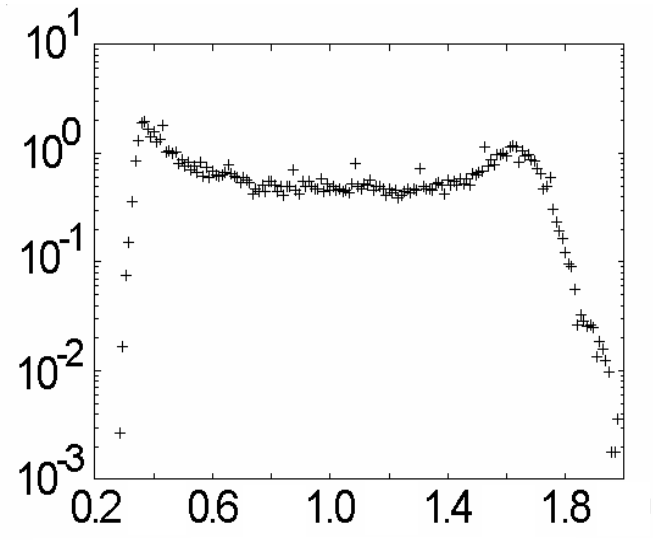

Fig. 3(d)

Figure 3. PDF(z) versus z for a retro-reflector spacing of 10 mm and one-way path length of 75 m. Receiver lens aperture diameters, D_R , were (a) – 3mm, (b) – 10mm, (c) – 20mm, and (d) – 30 mm.

The double peaked, or "U" shaped PDFs arise as follows. If both retro-reflectors are located within the same coherence volume, that is, the difference in optical path lengths to each reflector is less than a coherence length of the laser source and the transverse separation distance between the

reflectors is less than a lateral spatial coherence length of the atmospheric turbulence corrupted transmitter wavefronts, then constructive or destructive interference can be expected in the returned laser field. This experiment did not directly measure the mutual coherence function of the returned light. Instead it measured a PDF of the intensity fluctuations that indirectly recorded the presence of the interference. The total returned light intensity at the pupil plane of the receiver lens consisted of two log-normally fluctuating intensities, one from each retro-reflector, and a third component proportional to the product of the square roots of the two fluctuating intensities with $\cos(\phi)$ where ϕ is a randomly varying phase angle whose value depended on the difference in optical phase of the two returned light beams. The PDF for the total intensity is determined by the convolution of the individual PDFs for each of the three terms. The PDF for $\cos(\phi)$ is "U" shaped which gives the composite PDF its double peaked nature. The data of Figure 3 indicate that the optical field returned by the two closely spaced retro-reflectors contains substantial amounts of interference over a wide spatial area (up to at least 30 mm) under these experimental conditions.

As the spacing between the two retro-reflectors is increased, the shape of the PDF of the return light intensity changes and becomes log-normal once the spacing exceeds the lateral coherence distance of the transmitted optical field. This behavior is shown in Figures 4 (a)-(d) and 5(a)-(d).

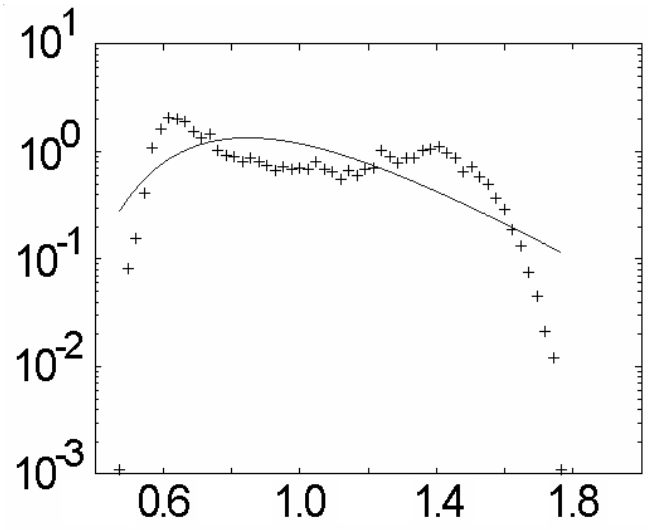

Fig. 4(a)

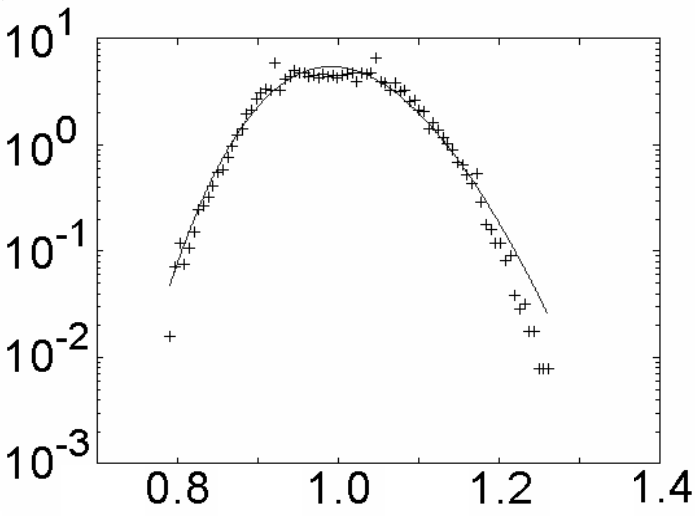

Fig. 4(b)

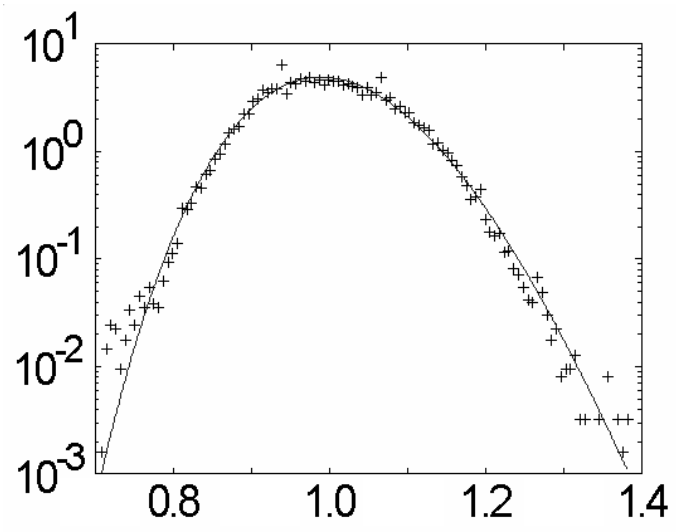

Fig. 4(c)

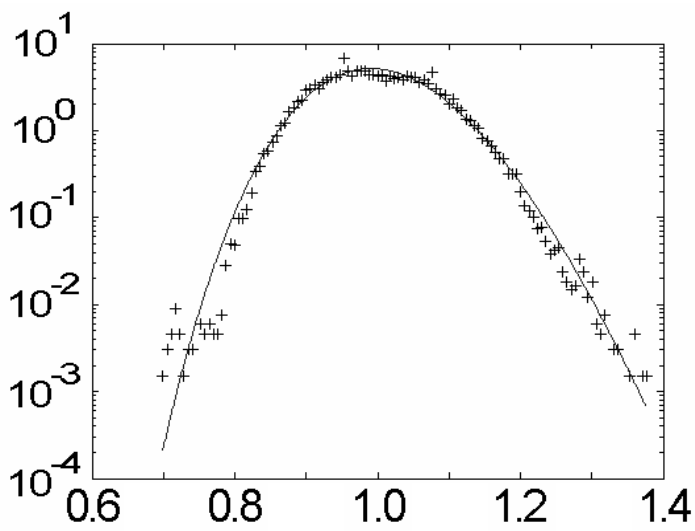

Fig. 4(d)

Figure 4. PDF(z) versus z for a retro-reflector spacing of 20 mm and one-way path length of 75 m. Parameter values are (a) D_R = 3mm, $\sigma^2_{\ln z} = 1.09x10^{-1}$, $\Delta z = 2.39x10^{-2}$; (b) D_R = 10mm, $\sigma^2_{\ln z} = 5.38x10^{-3}$, $\Delta z = 5.96x10^{-3}$, (c) D_R = 20mm, $\sigma^2_{\ln z} = 6.61x10^{-3}$, $\Delta z = 6.06x10^{-3}$, (d) D_R = 30mm, $\sigma^2_{\ln z} = 6.02x10^{-3}$, $\Delta z = 5.89x10^{-3}$ Solid curve denotes theoretical log-normal PDF with experimentally measured values of <lnz> and $\sigma^2_{\ln z}$.

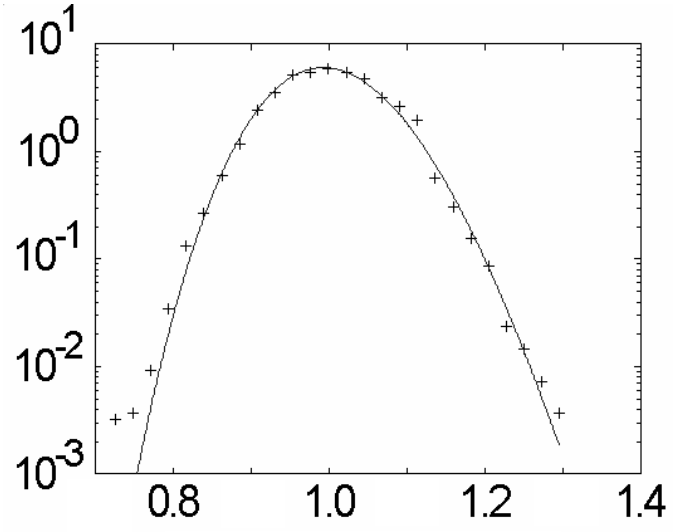

Fig. 5(a)

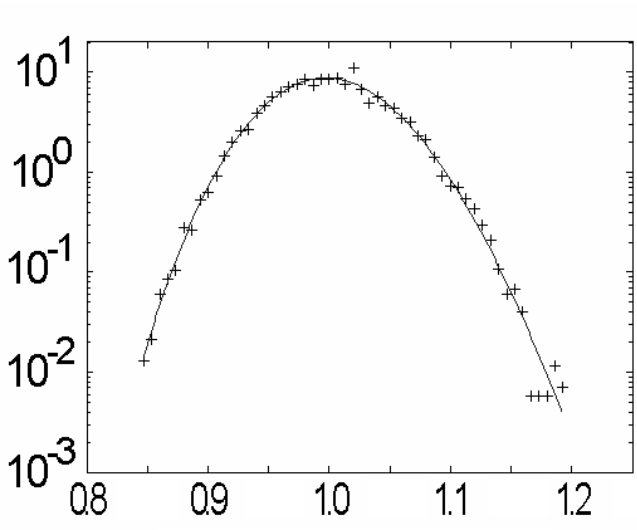

Fig. 5(b)

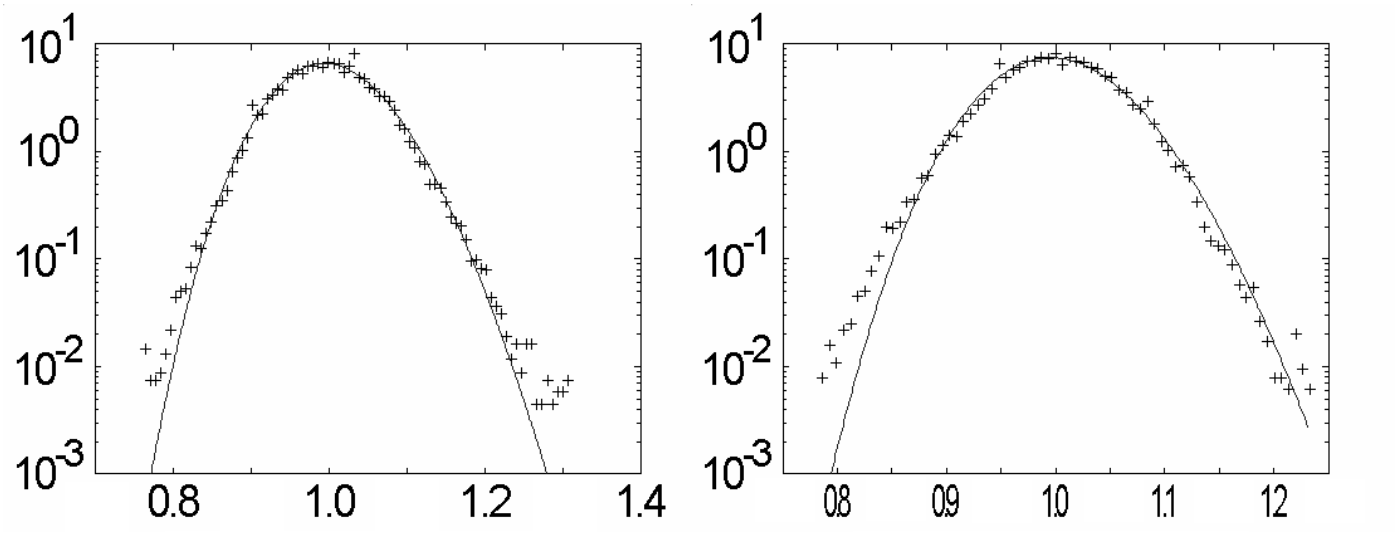

Fig. 5(c) Fig. 5(d)

Figure 5. PDF(z) versus z for a retro-reflector spacing of 60 mm and one-way path length of 75 m. Parameter values are (a) D_R = 3mm, $\sigma^2_{\ln z} = 4.36x10^{-3}$, $\Delta z = 2.28x10^{-2}$; (b) D_R = 10mm, $\sigma^2_{\ln z} = 2.07x10^{-3}$, $\Delta z = 6.65x10^{-3}$, (c) D_R = 20mm, $\sigma^2_{\ln z} = 3.63x10^{-3}$, $\Delta z = 6.52x10^{-3}$, (d) D_R = 30mm, $\sigma^2_{\ln z} = 2.84x10^{-3}$, $\Delta z = 6.47x10^{-3}$. Solid curve denotes theoretical log-normal PDF with experimentally measured values of <ln*z*> and $\sigma^2_{\ln z}$.

The transition to log-normal behavior as the retro-reflector spacing is increased is shown in Figures 4 and 5 with the lens aperture diameter as a parameter. These show the passage from always "double peaked" to always log-normal as the retro-reflector spacing is increased, and/or as the aperture diameter of the receiver focusing lens is increased. The solid lines in these figures represent a log-normal PDF as computed from equation (4) using values of $< \ln z >$ and $\sigma^2_{\ln z}$ determined directly from the data file. The values of $\sigma^2_{\ln z}$ among these plots represent the variation in values of C_n^2 from data file to data file. These ranged in value from about 1 x10^{-14} to about 5x10^{-14} m$^{-2/3}$ for the data files that fit a log-normal PDF model.

Figure 6 shows an experimentally measured PDF for the case of two retro-reflectors spaced 10 mm apart but separated by several centimeters in the beam propagation direction so that the retros were in different longitudinal coherence volumes. These PDFs were always log-normal, regardless of lens aperture diameter.

The measurements described above give an indirect indication of the lateral spatial coherence length of the beam at the retro-reflectors, through the dependence on retro-reflector spacing, and at the receiver through the behavior of the PDFs with aperture size. The mutual coherence function (or wave structure function) itself of the light is not directly measured. The theoretical spatial coherence length, under the assumption of a Kolmogorov spectrum, for a Gaussian beam can be found from the normalized mutual coherence function and is given by the approximate form [4]

$$\frac{\Gamma_2(d,L)}{\Gamma_2(0,L)} = \exp\left[-\frac{1}{4}\Lambda\left(\frac{kd^2}{L}\right) - \frac{3}{8}a\left(\frac{qkd^2}{L}\right)^{5/6}\right] \qquad (5)$$

where d is the transverse distance between the field points, L the optical path length, and k the wave vector. The other terms are $q = 1.22(\sigma_1^2)^{6/5}$, the Rytov variance $\sigma_1^2 = 1.23 C_n^2 k^{7/6} L^{11/6}$, $\Lambda = 2L/kW^2(L)$, $a = (1-\Theta^{8/3})/(1-\Theta)$, $\Theta = 1 + L/R(L)$ where the Gaussian beam waist and radius of curvature at distance L are denoted by $W^2(L)$ and $R(L)$, respectively. The lateral spatial coherence length is obtained by finding the value d_c that renders the argument of the exponential in eqn. (7) equal to – 1. The Gaussian beam used in these experiments had the values $\Theta = 2$ and $\Lambda = 4x10^{-3}$ at L = 75 m. Figure 7 shows the behavior of d_c as found from eqn. (5) over the range $10^{-15} \le C_n^2 \le 10^{-13}$. Figure 7 indicates the lateral coherence distance should be on the order of 15 to 55 mm and is very consistent with the behavior of the experimentally determined PDFs.

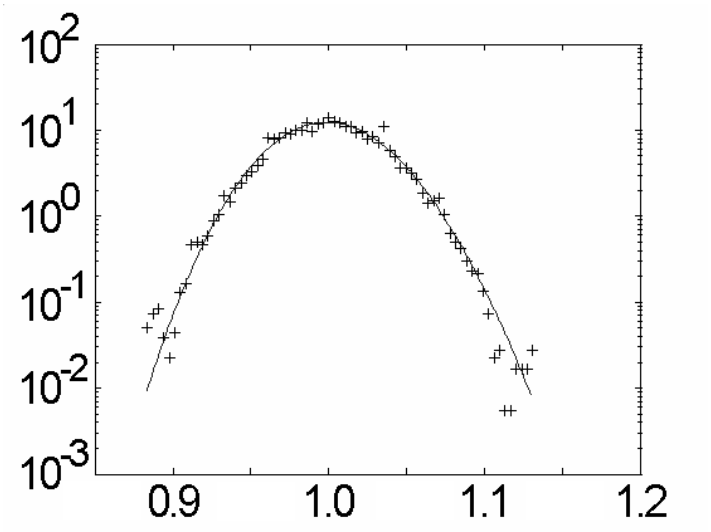

Figure 6. Experimentally determined PDF(z) versus z for light reflected by two retro-reflectors spaced 10 mm apart in the transverse direction and 3 cm apart in the beam propagation (longitudinal) direction

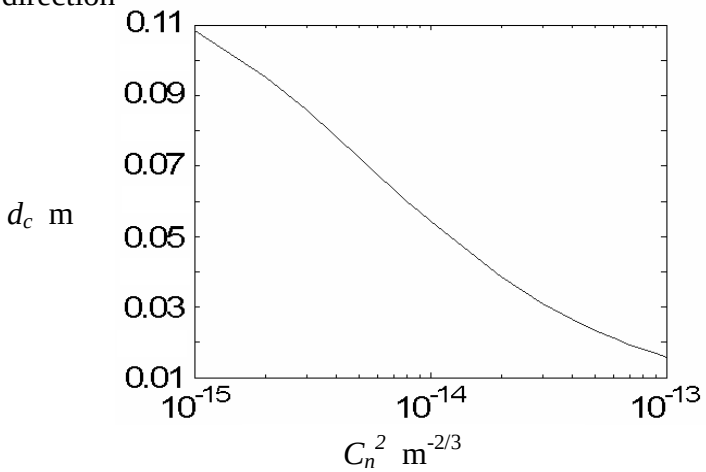

Figure 7. Lateral coherence length versus refractive index structure constant as computed from (5).

Finally, the behavior of variance of the intensity fluctuations of the retro-reflected light, irrespective of the form of the PDF, as a function of retro-reflector spacing is summarized in Figure 8 which plots normalized intensity variance, $\sigma_I^2 / < I >^2$, as determined directly from the data files, versus retro-reflector spacing for lens aperture diameters of 3, 5, 10, and 30 mm. If the PDF for the returned light intensity is log-normal, then $\sigma_I^2 / < I >^2 = \exp(4\sigma_\chi^2) - 1$ where $4\sigma_\chi^2 = \sigma_{\ln z}^2$. Figure 8 shows that in order to operate this system with minimal bit error rate, the retro-reflector spacing should be about 60 mm in order for $\sigma_I^2 / < I >^2$ to reach its minimal value on the order of 10^{-3} which will also result in a single peaked log-normal PDF for the normalized optical field intensity.

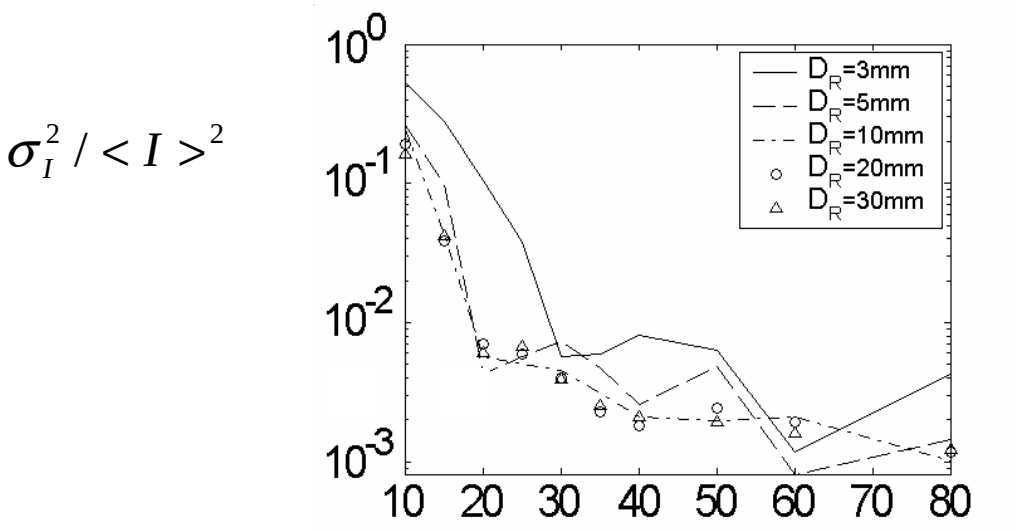

Figure 8. Experimentally measured values of normalized intensity variance $\sigma_I^2 / < I >^2$ as a function of retro-reflector spacing with lens aperture diameter as a parameter. For the log-normal PDFs, $\sigma_I^2 / < I >^2 = \exp(4\sigma_\chi^2) - 1$.

IV. Conclusions

The performance of an optical communication link that uses retromodulators depends heavily on the placement of the individual retro-reflectors in order to avoid excess intensity fluctuations that arise from coherent interference at the receiver between light beams reflected by the individual retro-reflectors. It is therefore desirable to use a laser beam that has a low coherence volume transmitted with minimal divergence angle so that the retro-reflectors can be closely spaced, yet located in independent coherence volumes. Broad line-width, 980 nm high power diode lasers appear to be a good candidate for use in these types of systems. The results of the experimental measurements to

determine lateral coherence distances reported here clearly show the evolution of the PDF of light intensity from broad, multiple peaked densities to single peaked lognormal densities with variance determined by both Gaussian beam parameters and the atmospheric turbulence levels as the spacing between the retro-reflectors increased until it exceeded the optical field lateral coherence length. The latter is determined by eqn. (5) and depends on Gaussian beam parameters at the plane of the retro-reflectors (beam waist, radius of curvature), optical path length, and turbulence levels. The particular laser used here had a coherence volume of approximately 6cms x 0.5 mm = 0.3 cm^3 after propagating 75 m through atmospheric turbulence characterized by values of C_n^2 in the range 10^{-13} to 10^{-14} $m^{-2/3}$

VI References

1. G.C. Gilbreath, W.S. Rabinovich, et. al., "Progress in development of multiple quantum well retromodulators for free-space data links", *Optical Engineering,* **42**(6), 1611-1617, (2003)
2. W.S. Rabinovich, , G. C. Gilbreath, R. Mahon, R. Burris, P. Goetz, C. I. Moore, M. Ferraro, J. L. Witdowsky, L. Swingen, E. Oh, J. Koplow, "Free-space optical communications link at 1550 nm using multiple quantum well modulating retro-reflectors over a 1-kilometer range", Opt.Soc.of Am Ann. Mtg., **230.5590**, May, 2003.
3. A. Papoulis and S. Pillai, *Probability, Random Variables, and Stochastic Processes, 4th ed.,* McGraw Hill, New York, (2002)pp.91-92.
4. L. Andrews and R. Phillips, *Laser beam Propagation through Random Media,* SPIE Optical Engineering Press, Bellingham, WA, (1998), Ch. 6.
5. L. Mandel and E. Wolf, *Optical Coherence and Quantum Optics,* Cambridge University Press, (1995), pp. 452-457.
6. W. Miller, J. Ricklin, and L. Andrews, "Log-amplitude variance and wave structure function: a new perspective for Gaussian beams", *J. Opt. Soc. Amer.*, **10**(4), 661-672, (1993).